JPE 16-3-24

http://dx.doi.org/10.6113/JPE.2016.16.3.1067
ISSN(Print): 1598-2092 / ISSN(Online): 2093-4718

Accurate Voltage Parameter Estimation for Grid Synchronization in Single-Phase Power Systems

Zhiyong Dai†, Hui Lin*, Yanjun Tian**, Wenli Yao*, and Hang Yin***

†,*School of Automation, Northwestern Polytechnical University, Xi'an, China
**Department of Energy Technology, Aalborg University, Aalborg, Denmark
***Institute of Energy and Automation Technology, Technology University of Berlin, Berlin, Germany

Abstract

This paper presents an adaptive observer-based approach to estimate voltage parameters, including frequency, amplitude, and phase angle, for single-phase power systems. In contrast to most existing estimation methods of grid voltage parameters, in this study, grid voltage is treated as a dynamic system related to an unknown grid frequency. Based on adaptive observer theory, a full-order adaptive observer is proposed to estimate voltage parameters. A Lyapunov function-based argument is employed to ensure that the proposed estimation method of voltage parameters has zero steady-state error, even when frequency varies or phase angle jumps significantly. Meanwhile, a reduced-order adaptive observer is designed as the simplified version of the proposed full-order observer. Compared with the frequency-adaptive virtual flux estimation, the proposed adaptive observers exhibit better dynamic response to track the actual grid voltage frequency, amplitude, and phase angle. Simulations and experiments have been conducted to validate the effectiveness of the proposed observers.

Key words: Adaptive observer, Grid synchronization, Voltage parameter estimation, Zero steady-state estimation error

I. INTRODUCTION

Grid voltage parameters, such as frequency, amplitude, and phase angle, are important information for many power system applications. In recent years, various estimation methods of grid voltage parameters have been proposed, such as discrete Fourier transform [1], [2], fast Fourier transform [3], Kalman filtering [4], zero-crossing detection [5], [6], least squares estimation [7], adaptive estimation [8], artificial neural networks [9], adaptive notch filter [10]–[13], complex vector filter [14], and phase-locked loop (PLL) [15], [16].

Among the aforementioned parameter estimation schemes, PLL has the capacity to achieve instantaneous tracking of single-phase grid voltage parameters. In addition, PLL has been the focus of considerable attention because of its more simple structure and good performance. In contrast to three-phase power systems, single-phase power systems have less information for generating quadrature signal waveforms, which are essential in PLL systems. A simple orthogonal signal generator (OSG), which is a transfer delay block, was designed in [17] to create a quadrature signal. However, when grid frequency deviates from its nominal value, generating an exact quadrature signal in the OSG is impossible, which introduces steady-state errors in frequency estimation [18]. Another OSG, the Hilbert transform-based OSG proposed in [19], shows good performance under optimum grid conditions. However, under frequency jump conditions, its performance degrades in terms of steady-state errors. Another solution for grid synchronization, known as second-order generalized integrator phase-locked loop (SOGI-PLL), was developed in [20]. Based on the second-order generalized integrator (SOGI), SOGI-PLL has a simple implementation and minor computing issues. However, SOGI-PLL suffers from a slow dynamic response because of the presence of filters. Several papers, such as [21] and [22], developed new SOGI-PLL structures combined with the adaptive observer method to address frequency jump faults. Thus, a better estimation performance is achieved when frequency varies. However, to linearize the output of the phase detector (PD), these methods, similar to most existing PLLs, are based on the assumption that the phase angle estimation

Manuscript received Mar. 6, 2015; accepted Dec. 28, 2015
Recommended for publication by Associate Editor Jaeho Choi.
†Corresponding Author: daizhiyong_nwpu@hotmail.com
Tel: +86-029-88431311, Fax: +86-029-88431311, Northwestern Polytechnical University
*School of Automation, Northwestern Polytechnical University, China
**Department of Energy Technology, Aalborg University, Denmark
***Inst. of Energy & Automation Tech., Tech. Univ. of Berlin, Germany

error is arbitrarily small [18]. However, when this assumption is unsatisfied, such as a significant phase angle jump, the performance of these PLLs will deteriorate. Moreover, the introduction of the SOGI filter causes a dynamic response loss in these estimation methods.

In this study, grid voltage is considered a dynamic system related to an unknown parameter, that is, grid frequency. Based on adaptive theory [23] and observer theory [24], a full-order adaptive observer is proposed to estimate grid voltage parameters. To simplify the proposed full-order observer, a reduced-order adaptive observer is developed by following a similar philosophy. Strict Lyapunov-based arguments ensure that the addressed observers are capable of tracking the actual grid voltage parameters with zero steady-state error.

In contrast to most existing estimation methods, the proposed adaptive observer method does not rely on PLL, which eliminates the possibility of the previously described assumption in the linearization of PD output that requires the phase angle estimation error to be arbitrarily small. Consequently, the proposed method can also estimate voltage parameters with zero steady-state error when a significant phase angle jump occurs. Moreover, compared with the frequency-adaptive virtual flux estimation proposed in [21], the proposed method exhibits better dynamic response and smaller overshoot.

This paper is organized as follows: A full-order adaptive observer-based parameter estimation of the grid voltage is proposed in Section II. As a simplified version of the full-order adaptive observer, a reduced-order adaptive observer-based grid voltage parameter estimation is proposed in Section III. MATLAB-based simulation results and dSPACE-based experimental results are provided in Sections IV and V, respectively. Finally, the conclusion is presented in Section VI.

II. Full-order Adaptive Observer-Based Grid Voltage Parameter Estimation

In a single-phase grid, grid voltage can be expressed as follows:

$$v = V_g \sin(\omega t + \phi) = V_g \sin\psi \,, \tag{1}$$

where V_g is the amplitude of the grid voltage, ω is the angular frequency of the grid voltage, and $\psi \in [0,2\pi)$ is the phase angle. Based on the relationship between the grid voltage and its derivative, the model of the grid voltage can be represented by the following expressions:

$$\begin{aligned} \dot{x} &= \bar{A}x \\ y &= Cx \end{aligned}, \tag{2}$$

where:

$$\bar{A} = \begin{bmatrix} 0 & 1 \\ -\theta & 0 \end{bmatrix} \text{ with } \theta = \omega^2 \,, \quad C = \begin{bmatrix} 1 & 0 \end{bmatrix}$$

$$x = \begin{bmatrix} x_1 \\ x_2 \end{bmatrix} = \begin{bmatrix} v \\ \dot{v} \end{bmatrix} = \begin{bmatrix} V_g \sin(\omega t + \phi) \\ V_g \omega \cos(\omega t + \phi) \end{bmatrix}.$$

According to system (2), the following relation exists:

$$rank\begin{bmatrix} C \\ C\bar{A} \end{bmatrix} = \begin{bmatrix} 1 & 0 \\ 0 & 1 \end{bmatrix} = 2 \,. \tag{3}$$

As a result, system (2) is observable. In this study, the grid voltage parameter estimation problem is reformulated as an adaptive estimation problem for the dynamic system (2) related to an unknown grid fundamental frequency ω. In the following section, an adaptive observer is proposed to estimate state x and fundamental frequency ω for system (2) with zero steady-state error. Based on the estimation of system state x and fundamental frequency ω, grid voltage parameters, including amplitude V_g, frequency ω, and phase angle ψ, are observed without steady-state estimation errors using Equation (21).

Initially, system (2) is rewritten as follows:

$$\begin{aligned} \dot{x} &= Ax - \begin{bmatrix} 0 \\ \theta \end{bmatrix} y \\ y &= Cx \end{aligned}, \tag{4}$$

where:

$$A = \begin{bmatrix} 0 & 1 \\ 0 & 0 \end{bmatrix}.$$

For the observable dynamic system (4), the full-order observer can be designed as follows:

$$\dot{\hat{x}} = A\hat{x} - \begin{bmatrix} 0 \\ \hat{\theta} \end{bmatrix} y + L(C\hat{x} - y), \quad \hat{x}(0) = x_0 \,, \tag{5}$$

where $\hat{x}$ is the estimation of the system state x and $\hat{\theta}$ is the estimation of the unknown parameter θ. Given that the linear system (4) is observable, matrix L exists to ensure that $A_c = A + LC$ is Hurwitz, which implies that $\exists P = P^T > 0$ and $Q = Q^T > 0$ such that:

$$A_c^T P + P A_c = -Q < 0 \,. \tag{6}$$

To facilitate development, the estimation errors can be defined as follows:

$$\begin{aligned} \tilde{x} &= \hat{x} - x \\ \tilde{\theta} &= \hat{\theta} - \theta \end{aligned}. \tag{7}$$

According to (4), (5), and (7), the estimation error dynamics can be expressed as follows:

$$\begin{aligned} \dot{\tilde{x}} &= A\tilde{x} - \begin{bmatrix} 0 \\ \tilde{\theta} \end{bmatrix} y + LC\tilde{x} \\ &= (\mathrm{A} + \mathrm{LC})\tilde{x} - \begin{bmatrix} 0 \\ \tilde{\theta} \end{bmatrix} y \cdot \\ &= A_c\tilde{x} - \begin{bmatrix} 0 \\ \tilde{\theta} \end{bmatrix} y \end{aligned} \tag{8}$$

Using the positive definite matrix P, we design the Lyapunov function as follows:

$$V(\tilde{x}, \tilde{\theta}) = \tilde{x}^T P \tilde{x} + \frac{1}{\gamma}\tilde{\theta}^2 \,, \tag{9}$$

where parameter $\gamma > 0$. The derivative of $V(\tilde{x}, \tilde{\theta})$ can be expressed as follows:

$$\begin{aligned}\dot{V}(\tilde{x},\tilde{\theta}) &= -\tilde{x}^T Q\tilde{x} - 2\tilde{x}^T P\begin{bmatrix}0\\ \tilde{\theta}\end{bmatrix} y + \frac{2}{\gamma}\tilde{\theta}\dot{\tilde{\theta}} \\ &= -\tilde{x}^T Q\tilde{x} - 2\tilde{x}^T P\begin{bmatrix}0\\ 1\end{bmatrix} y\tilde{\theta} + \frac{2}{\gamma}\tilde{\theta}\dot{\tilde{\theta}}\end{aligned} . \quad (10)$$

Given that θ is a constant, $\dot{\tilde{\theta}} = \dot{\hat{\theta}}$ can be deduced. The adaptive update law can be designed as follows:

$$\begin{aligned}\dot{\hat{\theta}} = \dot{\tilde{\theta}} &= \gamma\tilde{x}^T P\begin{bmatrix}0\\ 1\end{bmatrix} y \\ &= \gamma\begin{bmatrix}\hat{x}_1 - x_1 & \hat{x}_2 - x_2\end{bmatrix} P\begin{bmatrix}0\\ 1\end{bmatrix} y \\ &= \gamma\begin{bmatrix}\hat{x}_1 - x_1 & \hat{x}_2\end{bmatrix} P\begin{bmatrix}0\\ 1\end{bmatrix} y \\ &\quad -\gamma\begin{bmatrix}0 & x_2\end{bmatrix} P\begin{bmatrix}0\\ 1\end{bmatrix} y, \quad \hat{\theta}(0) = \hat{\theta}_0\end{aligned} . \quad (11)$$

According to system (2), the following relation exists:

$$x_1 = y \quad \text{and} \quad x_2 = \dot{x}_1 = \dot{y},$$

which leads to the following expression:

$$\begin{aligned}\dot{\hat{\theta}} &= \gamma\begin{bmatrix}\hat{x}_1 - y & \hat{x}_2\end{bmatrix} P\begin{bmatrix}0\\ 1\end{bmatrix} y \\ &\quad -\gamma\begin{bmatrix}0 & y\dot{y}\end{bmatrix} P\begin{bmatrix}0\\ 1\end{bmatrix}, \qquad \hat{\theta}(0) = \hat{\theta}_0\end{aligned} . \quad (12)$$

State variable l and its dynamics are introduced as follows:

$$\dot{l} = \gamma\begin{bmatrix}\hat{x}_1 - y & \hat{x}_2\end{bmatrix} P\begin{bmatrix}0\\ 1\end{bmatrix} y, \quad l(0) = l_0 . \quad (13)$$

Substituting (13) into (12) and taking the integral of both sides of (12) will yield the following expression:

$$\begin{aligned}\hat{\theta} &= l - \gamma\begin{bmatrix}0 & \frac{y^2}{2}\end{bmatrix} P\begin{bmatrix}0\\ 1\end{bmatrix} + \hat{\theta}(0) \\ &\quad -l(0) + \gamma\begin{bmatrix}0 & \frac{y(0)^2}{2}\end{bmatrix} P\begin{bmatrix}0\\ 1\end{bmatrix}\end{aligned} . \quad (14)$$

Specifically, by choosing:

$$\hat{\theta}(0) = l(0) - \gamma\begin{bmatrix}0 & \frac{y(0)^2}{2}\end{bmatrix} P\begin{bmatrix}0\\ 1\end{bmatrix},$$

the adaptive update law can be simplified as follows:

$$\hat{\theta} = l - \gamma\begin{bmatrix}0 & \frac{y^2}{2}\end{bmatrix} P\begin{bmatrix}0\\ 1\end{bmatrix}. \quad (15)$$

To prove observer stability and analyze the steady-state accuracy of the estimation, substituting (13) and (15) into the derivative of the Lyapunov function (10) can produce the following expression:

$$\dot{V}(\tilde{x},\tilde{\theta}) = -\tilde{x}^T Q\tilde{x} \le 0 . \quad (16)$$

Therefore, the closed-loop system formed by (8), (13), and (15) is globally stable. In the remainder of this section, the steady-state estimation error will be analyzed through LaSalle's invariance principle [23]. Initially, we examine LaSalle's invariance principle by setting:

$$\dot{V}(\tilde{x},\tilde{\theta}) = -\tilde{x}^T Q\tilde{x} = 0 .$$

Then, the following equation can be derived:

$$\begin{aligned}\tilde{x}_1 &= \hat{x}_1 - x_1 = 0 \\ \tilde{x}_2 &= \hat{x}_2 - x_2 = 0\end{aligned} . \quad (17)$$

Substituting (17) into the closed-loop system formed by (8), (13), and (15) will yield:

$$\begin{aligned}\tilde{\theta} y &= 0 \\ \dot{\tilde{\theta}} &= 0\end{aligned} . \quad (18)$$

Thus,

$$\tilde{\theta} = 0 . \quad (19)$$

Finally, the closed-loop system formed by (8), (13), and (15) is asymptotically stable through LaSalle's invariance principle, which implies that the full-order adaptive observer will yield:

$$\begin{aligned}\lim_{t\to\infty}\tilde{x} &= \lim_{t\to\infty}(\hat{x} - x) = 0 \\ \lim_{t\to\infty}\tilde{\theta} &= \lim_{t\to\infty}(\hat{\theta} - \theta) = 0\end{aligned} . \quad (20)$$

In other words, the estimation of system state x and unknown parameter θ has zero steady-state error. With the aid of state estimation $\hat{x}$ and unknown parameter estimation $\hat{\theta}$, voltage frequency ω, voltage amplitude V_g, and voltage phase angle ψ can be estimated as follows:

$$\hat{\omega} = \sqrt{\hat{\theta}}, \quad \hat{V}_g = \sqrt{\hat{x}_1^2 + \frac{\hat{x}_2^2}{\hat{\omega}^2}} \quad \text{and} \quad \psi = \arctan\left(\frac{x_1\hat{\omega}}{\hat{x}_2}\right). \quad (21)$$

Clearly, with property (20) and the relationships expressed (21), the proposed full-order adaptive observer in this section can track the actual grid voltage parameters, including frequency, amplitude, and phase angle, with zero steady-state error.

In summary, the proposed full-order adaptive observer formed by (5), (13), (15), and (21) can be clearly described in Fig. 1. In the figure, the thick lines represent the vector variables, whereas the thin lines represent the scalar variables.

III. Reduced-order Adaptive Observer-based Grid Voltage Parameter Estimation

The full-order adaptive observer proposed in the previous section is three-dimensional. A two-dimensional reduced-order adaptive observer is developed in this section to simplify parameter estimation. With the aid of linear reduced-order observer theory, the linear reduced-order observer for system (4) is designed as follows:

$$\begin{aligned}\dot{z} &= -\alpha z - \left(\hat{\theta} + \alpha^2\right) y, \quad z(0) = z_0 \\ \hat{x}_2 &= z + \alpha y\end{aligned} , \quad (22)$$

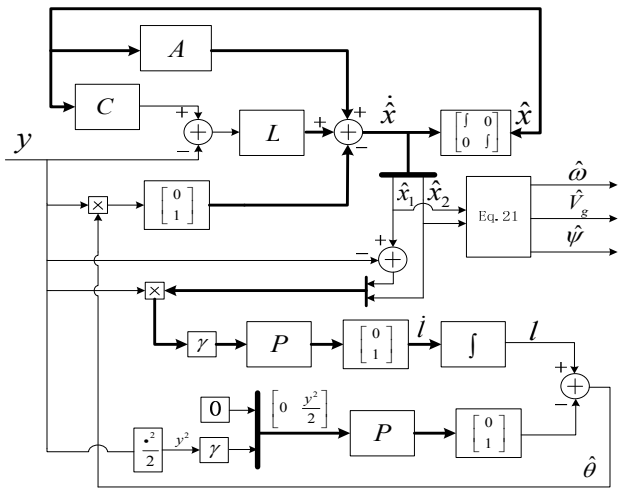

Fig. 1. Structure of the full-order adaptive observer.

where $z \in R$ is the state variable, $\hat{x}_2$ is the estimation of the system state x_2, and the parameter $\alpha > 0$. The estimation error $\tilde{x}_2$ is introduced as follows:

$$\tilde{x}_2 = \hat{x}_2 - x_2 . \tag{23}$$

According to the linear system (4) and the reduced-order observer (22), the estimation error dynamics can be deduced as follows:

$$\begin{aligned} \dot{\tilde{x}}_2 &= -\alpha\tilde{x}_2 - \hat{\theta}y - \dot{x}_2 \\ &= -\alpha\tilde{x}_2 - y\tilde{\theta} \end{aligned} . \tag{24}$$

Then, we construct the following Lyapunov function:

$$U(\tilde{x}_2, \tilde{\theta}) = \frac{1}{2}\tilde{x}_2^2 + \frac{1}{2\beta}\tilde{\theta}^2 , \tag{25}$$

where parameter $\beta > 0$. Based on (24) and (25), the following relation can be deduced:

$$\dot{U}(\tilde{x}_2, \tilde{\theta}) = -\alpha\tilde{x}_2^2 - y\tilde{x}_2\tilde{\theta} + \frac{1}{\beta}\dot{\tilde{\theta}}\tilde{\theta} . \tag{26}$$

With a philosophy similar to that in the previous section, the adaptive update law can be developed as follows:

$$\begin{aligned} \dot{\hat{\theta}} &= \dot{\tilde{\theta}} = \beta\tilde{x}_2 y \\ &= \beta\hat{x}_2 y - \beta x_2 y, \quad \hat{\theta}(0) = \hat{\theta}_0 \end{aligned} . \tag{27}$$

According to system (2), the following relation exists:

$$x_2 = \dot{x}_1 = \dot{y} .$$

Thus, the following expression can be rendered:

$$\dot{\hat{\theta}} = \beta\hat{x}_2 y - \beta y\dot{y}, \quad \hat{\theta}(0) = \hat{\theta}_0 . \tag{28}$$

We introduce the state variable $\eta \in R$; its dynamics can be expressed as follows:

$$\dot{\eta} = \beta\hat{x}_2 y, \quad \eta(0) = \eta_0 . \tag{29}$$

By substituting (29) into (28) and taking the integral of both sides of (28), the following equation can be derived:

$$\hat{\theta} = \eta - \frac{\beta}{2}y^2 + \hat{\theta}(0) - \eta(0) + \frac{\beta}{2}y(0)^2 . \tag{30}$$

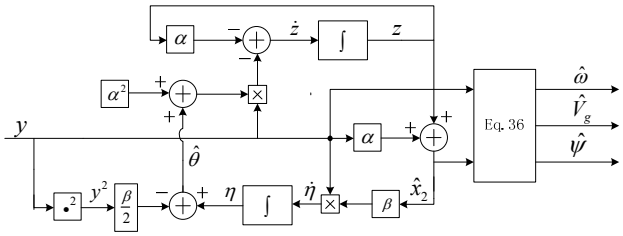

Fig. 2. Structure of the reduced-order adaptive observer.

Specifically, by choosing:

$$\hat{\theta}(0) = \eta(0) - \frac{\beta}{2}y(0)^2 ,$$

the adaptive update law can be deduced as follows:

$$\hat{\theta} = \eta - \frac{\beta}{2}y^2 . \tag{31}$$

Based on (26), (29), and (31), the derivative of $U(\tilde{x}_2, \tilde{\theta})$ can be expressed as follows:

$$\dot{U}(\tilde{x}_2, \tilde{\theta}) = -\alpha\tilde{x}_2^2 \le 0 . \tag{32}$$

As a result, the closed-loop system formed by (24), (29), and (31) is globally stable. LaSalle's invariance principle is applied to prove the asymptotic stability of the closed-loop system and to analyze the steady-state estimation error. By examining:

$$\dot{U}(\tilde{x}_2, \tilde{\theta}) = -\alpha\tilde{x}_2^2 = 0 , \tag{33}$$

$\tilde{x}_2 = 0$ can be easily deduced. Combining this with (24), (29), and (31) will lead to:

$$\begin{aligned} \tilde{x}_2 y &= 0 \\ \dot{\tilde{\theta}} &= 0 \end{aligned} , \tag{34}$$

which implies that $\tilde{\theta} = 0$. Through LaSalle's invariance principle, the closed-loop system formed by (24), (29), and (31) is asymptotically stable. In other words, the reduced-order adaptive observer achieves the following expression:

$$\begin{aligned} \lim_{t\to\infty}\tilde{x}_2 &= \lim_{t\to\infty}(\hat{x}_2 - x_2) = 0 \\ \lim_{t\to\infty}\tilde{\theta} &= \lim_{t\to\infty}(\hat{\theta} - \theta) = 0 \end{aligned} . \tag{35}$$

Correspondingly, the grid voltage parameters can be estimated as follows:

$$\begin{aligned} \hat{\omega} &= \sqrt{\hat{\theta}} \\ \hat{V}_g &= \sqrt{x_1^2 + \frac{\hat{x}_2^2}{\hat{\omega}^2}} = \sqrt{y^2 + \frac{\hat{x}_2^2}{\hat{\omega}^2}} \\ \psi &= \arctan\left(\frac{x_1\hat{\omega}}{\hat{x}_2}\right) = \arctan\left(\frac{y\hat{\omega}}{\hat{x}_2}\right) \end{aligned} . \tag{36}$$

Evidently, based on (35) and (36), the reduced-order adaptive observer proposed in this section can estimate grid voltage parameters with zero steady-state error.

In summary, the reduced-order adaptive observer proposed in this section has four parts, namely, (22), (29), (31), and (36). Fig. 2 illustrates its structure. The reduced-order adaptive observer is clearly a simpler version of the full-order adaptive observer.

IV. Simulation Results

The performance of the adaptive observer method for estimating single-phase grid voltage parameters is verified in this section. Through MATLAB/SIMULINK, the simulation results are provided in continuous time mode.

A. Full-order Adaptive Observer

Based on Fig. 1, the proposed full-order adaptive observer is implemented in MATLAB. The parameters of the observer are as follows:

$$L = \begin{bmatrix} -6\omega_r & -9\omega_r^2 \end{bmatrix}^T \quad \text{and} \quad \gamma = 20,$$

where the nominal grid frequency ω_r = 2π × 60 rad/s. Performance is analyzed under three different grid voltage fault cases, namely, frequency jump, amplitude jump, and phase angle jump.

1) Frequency Jump: Grid voltage is initially formed by $110\sqrt{2}\sin(120\pi t)$ V. With a frequency jump of 6 Hz at 5 s, the grid voltage is changed to $110\sqrt{2}\sin(132\pi t)$ V. Fig. 3 shows the parameter estimation results of the full-order adaptive observer, including (from top to bottom) the grid voltage *v*, estimated angular frequency $\hat{\omega}$, estimated amplitude $\hat{V}_g$, and estimated phase angle $\hat{\psi}$. After a relatively short transient, the estimated signals (solid lines) return to the actual parameters of the grid voltage (dotted lines) with zero steady-state error. For instance, the estimated frequency tracks the actual voltage frequency to 132π rad/s after one and a half cycles. With voltage disturbance on the frequency jump, a small transient disturbance also occurs at the estimated amplitude, which is finally fixed to the actual amplitude of the voltage. Moreover, the estimated phase angle perfectly follows the actual voltage phase angle after an almost imperceptible transient.

2) Amplitude Jump: Grid voltage is initially formed by $110\sqrt{2}\sin(120\pi t)$ V. With an amplitude jump of $-11\sqrt{2}$ V at 5 s, the grid voltage is changed to $99\sqrt{2}\sin(120\pi t)$ V. Fig. 4 shows the parameter estimation results of the full-order adaptive observer. Under this amplitude jump condition, the voltage estimated parameters (solid lines) track the actual voltage parameters (dotted lines) without steady-state error after a small transient. For instance, the estimated frequency has a small transient disturbance and returns to the desired actual frequency (120π rad/s) because of amplitude disturbance. Correspondingly, after a quarter cycle transient process, the estimated amplitude is fixed to the actual amplitude ($99\sqrt{2}$ V). Moreover, the amplitude jump has an imperceptible effect on phase angle estimation.

3) Phase Angle Jump: Grid voltage is initially formed by $110\sqrt{2}\sin(120\pi t)$ V. With a phase angle jump of π/6 rad at 5 s, the grid voltage is changed to $110\sqrt{2}\sin(120\pi t + \pi/6)$ V.

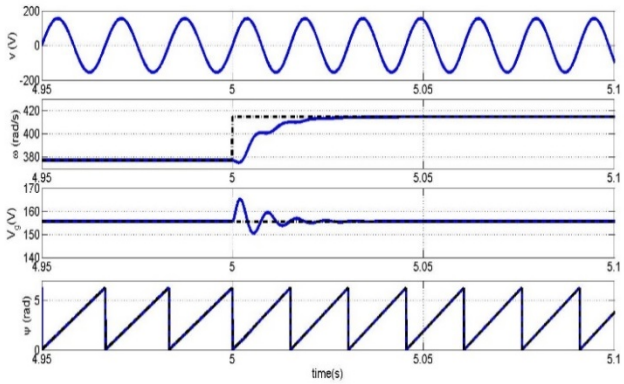

Fig. 3. Performance of the full-order adaptive observer with frequency jump. From top to bottom: estimated frequency $\hat{\omega}$, amplitude $\hat{V}_g$, and phase angle $\hat{\psi}$.

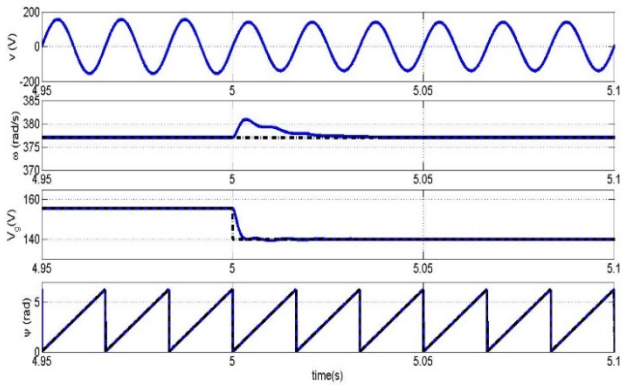

Fig. 4. Performance of the full-order adaptive observer with amplitude jump. From top to bottom: estimated frequency $\hat{\omega}$, amplitude $\hat{V}_g$, and phase angle $\hat{\psi}$.

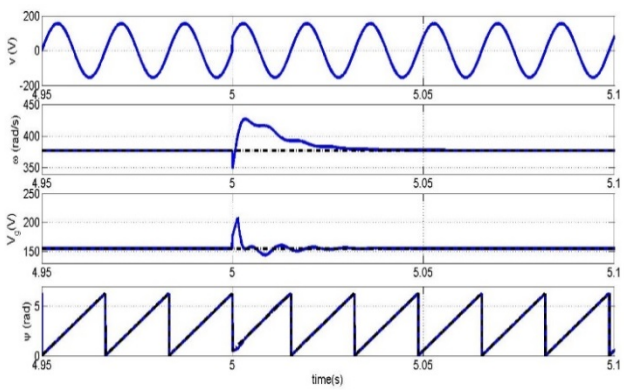

Fig. 5. Performance of the full-order adaptive observer with phase angle jump. From top to bottom: estimated frequency $\hat{\omega}$, amplitude $\hat{V}_g$, and phase angle $\hat{\psi}$.

Fig. 5 shows the parameter estimation results of the full-order adaptive observer. Under this phase angle jump condition, the voltage estimated parameters (solid lines) track the actual voltage parameters (dotted lines) with zero steady-state error after a small transient. For instance, the estimated frequency and amplitude have small transient disturbances and return to the desired actual frequency of 120π rad/s and amplitude of $110\sqrt{2}$ V, respectively. After a small transient period, the

estimated phase angle has zero steady-state error to track the actual phase angle.

B. Reduced-order Adaptive Observer

Based on Fig. 2, the reduced-order adaptive observer is established in MATLAB/SIMULINK with the following parameters:

$$\alpha = 1.6\omega_r \quad \text{and} \quad \beta = 10,$$

where the nominal grid frequency ω_r = 2π × 60 rad/s. Performance is also verified under three different grid voltage fault conditions, namely, frequency jump, amplitude jump, and phase angle jump.

1) Frequency Jump: With frequency jump of 6 Hz at 5 s, the grid voltage is changed from $110\sqrt{2}\sin(120\pi t)$ V to $110\sqrt{2}\sin(132\pi t)$ V. Fig. 6 shows the parameter estimation results of the reduced-order adaptive observer. Under this grid fault condition, the voltage estimated parameters (solid lines), including frequency, amplitude, and phase angle, have zero steady-state error to track the actual voltage parameters (dotted lines). For instance, after one and a half cycles, the estimated frequency is fixed to the actual voltage frequency (132π rad/s). The estimated amplitude has a small transient disturbance and ultimately returns to the desired actual amplitude because of the disturbance in the frequency jump. Moreover, the frequency jump almost has no effect on phase angle tracking.

2) Amplitude Jump: With an amplitude jump of $-11\sqrt{2}$ V at 5 s, the grid voltage is changed from $110\sqrt{2}\sin(120\pi t)$ V to $99\sqrt{2}\sin(120\pi t)$ V. Fig. 7 shows the parameter estimation results of the reduced-order adaptive observer. Under this grid fault condition, after a short transient process, the voltage estimated parameters (solid lines) return to the actual voltage parameters (dotted lines) with zero steady-state error. For instance, under the amplitude jump disturbance, the estimated frequency returns to 120π rad/s after one and a half cycles. Correspondingly, the estimated amplitude tracks the actual voltage amplitude after a small transient. Moreover, the estimated phase angle follows the actual phase angle well after an almost imperceptible transient.

3) Phase Angle Jump: With a phase angle jump of π/6 rad at 5 s, the grid voltage is changed from $110\sqrt{2}\sin(120\pi t)$ V to $110\sqrt{2}\sin(120\pi t + \pi/6)$ V. Fig. 8 shows the parameter estimation results of the reduced-order adaptive observer. After a short transient process, the estimated parameters (solid lines) track the actual voltage parameters (dotted lines) perfectly. For instance, after a short transient process, the estimated frequency and amplitude return to the desired actual frequency (120π rad/s) and amplitude ($110\sqrt{2}$ V), respectively. Moreover, phase angle estimation exhibits a rapid dynamic response and good steady-state accuracy.

In summary, based on the simulation results of the proposed full-order adaptive observer and reduced-order adaptive observer, the proposed adaptive estimation scheme has zero steady-state error to estimate grid voltage parameters when the frequency, amplitude, or phase angle of the grid voltage significantly changes. Moreover, this estimation method exhibits good dynamic performance in terms of setting time and overshoot.

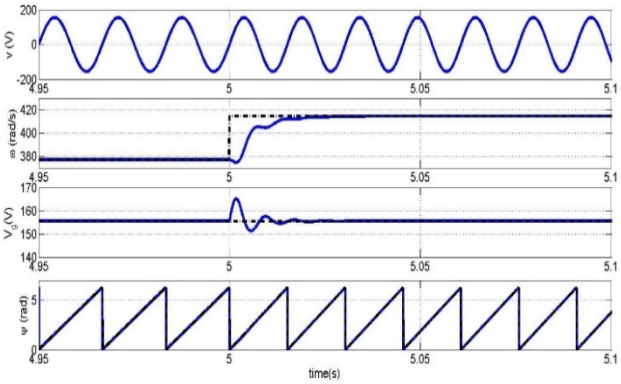

Fig. 6. Performance of the reduced-order adaptive observer with frequency jump. From top to bottom: estimated frequency $\hat{\omega}$, amplitude $\hat{V}_g$, and phase angle $\hat{\psi}$.

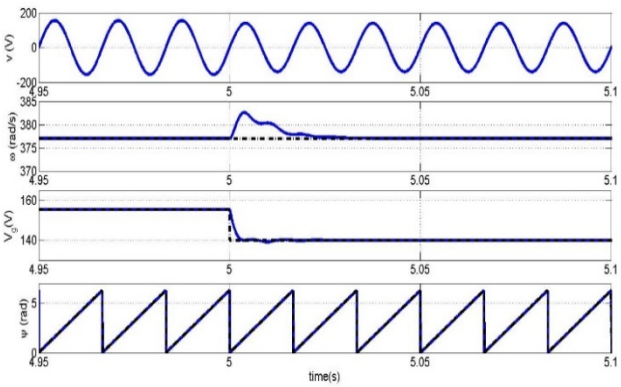

Fig. 7. Performance of the reduced-order adaptive observer with amplitude jump. From top to bottom: estimated frequency $\hat{\omega}$, amplitude $\hat{V}_g$, and phase angle $\hat{\psi}$.

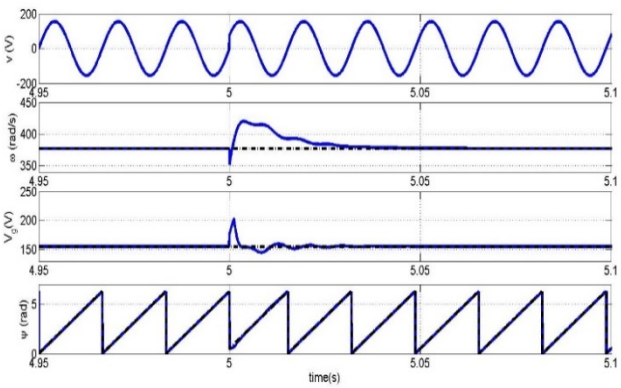

Fig. 8. Performance of the reduced-order adaptive observer with phase angle jump. From top to bottom: estimated frequency $\hat{\omega}$, amplitude $\hat{V}_g$, and phase angle $\hat{\psi}$.

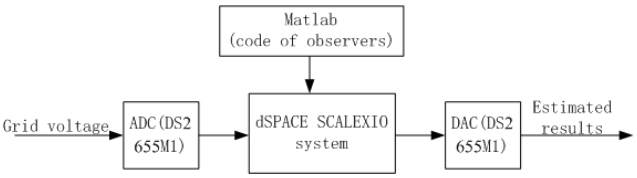

Fig. 9. Structure of the experimental system.

V. Experimental Results

The full-order adaptive observer and reduced-order adaptive observer proposed in this study are discretized with the step of 100 μs to implement the adaptive observer method on dSPACE using the discrete tool of MATLAB. Then, we rebuild the discrete observers into real-time codes and download the codes into dSPACE SCALEXIO. The control frequency of dSPACE is set as 10 kHz. Input signal acquisition and estimation result display use 14 bit ADCs/DACs, DS2655M1. The structure of the experimental system is shown in Fig. 9.

The selected parameters of the proposed adaptive observers are the same as that in the simulation cases (provided in the previous section). The experimental results based on the frequency-adaptive virtual flux estimation [21] are compared simultaneously. Fig. 10 shows the grid voltage, estimated frequency, amplitude, and phase angle. In the figure, the purple line represents the actual grid voltage; the blue, green, and red lines represent the parameter estimations based on the frequency-adaptive virtual flux estimation, full-order adaptive observer, and reduced-order adaptive observer, respectively.

The grid voltage is initially expressed as $110\sqrt{2}(\sin 120\pi t)$ V. With frequency jump, amplitude jump, and phase angle jump applied simultaneously, the grid voltage changes to $99\sqrt{2}\sin(132\pi t+\pi/6)$ V. The proposed voltage parameter observers are observed to have zero steady-state estimation error. Compared with the frequency-adaptive virtual flux estimation, the adaptive observers proposed in this study exhibit better dynamic response and smaller overshoot. More quantitative comparisons are shown in Table I.

VI. Conclusion

In this study, adaptive observers, including full-order and reduced-order adaptive observers, are proposed for the estimation of single-phase grid voltage parameters. Compared with most existing estimation methods of grid voltage parameters, in this study, grid voltage is regarded as a dynamic system related to an unknown parameter, that is, grid frequency. Moreover, strict Lyapunov function-based arguments ensure that parameter estimation of the grid voltage has zero steady-state error, even when frequency, amplitude, and/or phase angle jumps occur. An important feature of this method is that these proposed adaptive observers do not rely on linearization of the PD output, which eliminates the assumption

(a) Grid voltage (vertical scale. 50 V/div; horizontal scale, 20 ms/div).

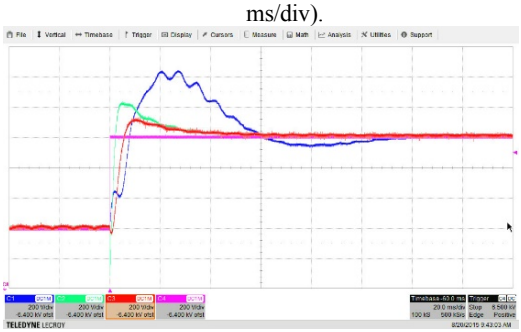

(b) Frequency estimation—purple line: actual grid voltage parameter; blue line: frequency-adaptive virtual flux estimation; green line: full-order adaptive observer; red line: reduced-order adaptive observer (vertical scale, $2\pi \times 2$ rad·s^{-1}/div; horizontal scale, 20 ms/div).

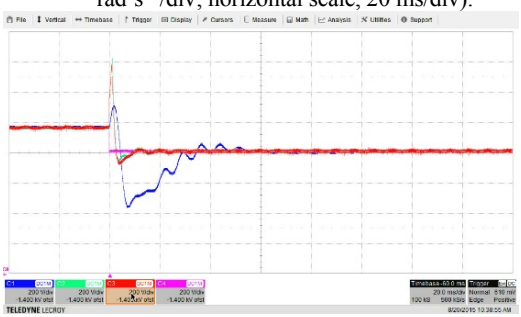

(c) Amplitude estimation—purple line: actual grid voltage parameter; blue line: frequency-adaptive virtual flux estimation; green line: full-order adaptive observer; red line: reduced-order adaptive observer (vertical scale, 20 V/div; horizontal scale, 20 ms/div).

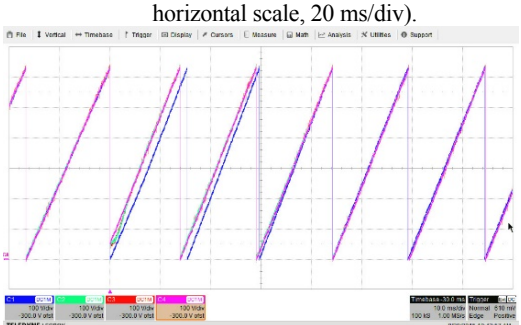

(d) Phase angle estimation—purple line: actual grid voltage parameter; blue line: frequency-adaptive virtual flux estimation; green line: full-order adaptive observer; red line: reduced-order adaptive observer (vertical scale, 1 rad/div; horizontal scale, 10 ms/div).

Fig. 10. Experimental performance comparison of the frequency-adaptive virtual flux estimation, the full-order adaptive observer, and the reduced-order adaptive observer.

TABLE I
PERFORMANCE COMPARISON OF THE FREQUENCY-ADAPTIVE VIRTUAL FLUX ESTIMATION, THE PROPOSED FULL-ORDER ADAPTIVE OBSERVER, AND THE REDUCED-ORDER ADAPTIVE OBSERVER

		Frequency-adaptive virtual flux estimation	Full-order adaptive observer	Reduced-order adaptive observer
Frequency estimation	2% setting time	47 ms	13 ms	5 ms
	Overshoot	6.67%	3.38%	1.59%
Amplitude estimation	2% setting time	53 ms	9 ms	8 ms
	Overshoot	25.7%	4.38%	4.99%
Phase angle estimation	2% setting time	92 ms	12 ms	9 ms
	Overshoot	20%	6.49%	3.82%

on the limitation of the initial phase angle estimation error. This feature ensures zero steady-state estimation error in the adaptive observers when the phase angle of the grid voltage jumps significantly. Moreover, from comparative experiments, the proposed adaptive observers exhibit better estimation performance in terms of dynamic response and overshoot.

ACKNOWLEDGMENT

This work was supported in part by the NSF of China under Grant No. 51407143, Specialized Research Fund for the Doctoral Program of Higher Education of China under Grant No. 20136102120049, Fundamental Research Funds for the Central Universities under Grant No. 3102014JCQ01066, and NSF of Shaanxi Province, China under Grant Nos. 2015JM5227 and 2014JQ7264.

REFERENCES

[1] M. S. Reza, M. Ciobotaru, and V. G. Agelidis, "Accurate estimation of single-phase grid voltage parameters under distorted conditions," *IEEE Trans. Power Del.,* Vol. 29, No. 3, pp. 1138-1146, Jun. 2014.

[2] E. Jacobsen and R. Lyons, "The sliding dft," *IEEE Signal Process. Mag.*, Vol. 20, No. 2, pp. 74-80, Mar. 2003.

[3] A. A. Girgis and F. M. Ham, "A quantitative study of pitfalls in the fft," *IEEE Trans. Aerosp. Electron. Syst.*, Vol. AES-16, No. 4, pp. 434-439, Jul. 1980.

[4] A. Routray, A. K. Pradhan, and K. P. Rao, "A novel kalman filter for frequency estimation of distorted signals in power systems," *IEEE Trans. Instrum. Meas.*, Vol. 51, No. 3, pp. 469-479, Jun. 2002.

[5] O. Vainio and S. J. Ovaska, "Noise reduction in zero crossing detection by predictive digital filtering," *IEEE Trans. Ind. Electron.*, Vol. 42, No. 1, pp. 58-62, Feb. 1995.

[6] O. Vainio, S. J. Ovaska, and M. Polla, "Adaptive filtering using multiplicative general parameters for zero-crossing detection," *IEEE Trans. Ind. Electron.*, Vol. 50, No. 6, pp. 1340-1342, Dec. 2003.

[7] H.-S. Song, K. Nam, and P. Mutschler, "Very fast phase angle estimation algorithm for a single-phase system having sudden phase angle jumps," in *37th Annual Meeting, Industry Applications conference(IAS),* Vol. 2, pp. 925-931, 2002.

[8] L. L. Lai, W. L. Chan, C. T. Tse, and A. T. P. So, "Real-time frequency and harmonic evaluation using artificial neural networks," *IEEE Trans. Power Del.*, Vol. 14, No. 1, pp. 52-59, Jan. 1999.

[9] Z. Y. Dai, W. Lin, and H. Lin, "Estimation of single-phase grid voltage parameters with zero steady-state error," *IEEE Trans. Power Electron.*, Vol. 31, No. 5, pp. 3867-3879, Jul. 2015.

[10] D. Yazdani, A. Bakhshai, G. Joos, and M. Mojiri, "A nonlinear adaptive synchronization techniquefor grid connected distributed energy sources," *IEEE Trans. Power Electron.*, Vol. 23, No. 4, pp. 2181-2186, Jul. 2008.

[11] M. Mojiri and A. R. Bakhshai, "Estimation of frequencies using adaptive notch filter," *IEEE Trans. Circuits Syst. II, Exp. Briefs*, Vol. 54, No. 4, pp. 338-342, Apr. 2007.

[12] K.-J. Lee, J.-P. Lee, D. Shin, D.-W. Yoo, and H.-J. Kim, "A novel grid synchronization pll method based on adaptive lowpass notch filter for grid-connected pcs," *IEEE Trans. Ind. Electron.*, Vol. 61, No. 1, pp. 292-301, Jan. 2014.

[13] G. Yin, L. Guo, and X. Li, "An amplitude adaptive notch filter for grid signal processing," *IEEE Trans. Power Electron.,* Vol. 28, No. 6, pp. 2638-2641, Jun. 2013.

[14] W. Li, X. Ruan, X. Wang, and D. Pan, "Grid synchronization systems of three-phase grid-connected power converters: a complex-vector-filter perspective," *IEEE Trans. Ind. Electron.*, Vol. 61, No. 4, pp. 1855-1870, Apr. 2014.

[15] S. Golestan, M. Monfared, F. D. Freijedo, and J. M. Guerrero, "Performance improvement of a pre-filtered synchronous-referenceframe pll by using a pid-type loop filter," *IEEE Trans. Ind. Electron.*, Vol. 61, No. 7, pp. 3469-3479, Jul. 2014.

[16] S. Golestan, M. Monfared, F. D. Freijedo, and J. M. Guerrero, "Dynamics assessment of advanced single-phase pll structures," *IEEE Trans. Ind. Electron.*, Vol. 60, No. 6, pp. 2167-2177, Jun. 2013.

[17] R. Zhang, M. Cardinal, P. Szczesny, and M. Dame, "A grid simulator with control of single-phase power converters in dq rotating frame," in *IEEE 33rd Annual Power Electronics Specialists Conference(PESC),* Vol. 3, pp. 1431-1436, 2002.

[18] R. Teodorescu, M. Liserre, and P. Rodriguez, *Grid Converters for Photovoltaic and Wind Power Systems*, John Wiley & Sons, Chap. 4, 2011.

[19] M. Saitou and T. Shimizu, "Generalized theory of instantaneous active and reactive powers in single-phase circuits based on hilbert transform," in *IEEE 33rd Annual Power Electronics Specialists Conference(PESC),* Vol. 3, pp. 1419-1424, 2002.

[20] M. Ciobotaru, R. Teodorescu, and F. Blaabjerg, "A new singlephase pll structure based on second order

generalized integrator," in *37th IEEE Power Electronics Specialists Conference(PESC),* pp. 1-6, 2006.
[21] J. A. Suul, A. Luna, P. Rodriguez, and T. Undeland, "Frequency-adaptive virtual flux estimation for grid synchronization under unbalanced conditions," in *36th Annual Conference on IEEE Industrial Electronics Society (IECON)*, pp. 486-492, Nov. 2010.
[22] A. Luna, C. Citro, C. Gavriluta, J. Hermoso, I. Candela, and P. Rodriguez, "Advanced PLL structures for grid synchronization in distributed generation," *in International Conference on Renewable Energies and Power Quality (ICREPQ)*, pp. 2769-2776, Mar. 2012.
[23] H. K. Khalil and J. Grizzle, *Nonlinear systems*, Prentice Hall, Upper Saddle River, Chap. 4, 2002
[24] W. J. Rugh, *Linear system theory*, 2th edition, Prentice Hall, Upper Saddle River, Chap. 4, 1996.

Zhiyong Dai was born in Xi'an, China in 1987. He received his B.S. and M.S. degrees in electrical engineering from Northwestern Polytechnical University, Xi'an, China in 2009 and 2012, respectively. He is currently working toward his Ph.D. degree in Detection Technology and Automation Device. Since 2014, he is a visiting student at the Department of Electrical Engineering and Computer Science, Case Western Reserve University, Cleveland, OH, USA. His research interests include power electronics, smart grid, power system control, and electric vehicles.

Hui Lin received his B.S. and M.S. degrees in electrical engineering and Ph.D. degree in control science engineering from Northwestern Polytechnical University, Xi'an, China in 1982, 1985, and 1993, respectively. He is currently a Professor at the Department of Electrical Engineering, Northwestern Polytechnical University. His teaching responsibilities and research interests are in the areas of power electronics, electric vehicles, motion control, and control theory.

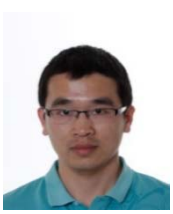

Yanjun Tian received his B.Sc. and M.Sc. degrees in electrical engineering from the Yanshan University, Qinhuangdao, China in 2009 and 2012, respectively. He is currently working toward his PhD degree in the Department of Energy Technology, Aalborg University Denmark. His research interests include distributed generation and active distribution network control focusing on impedance interaction, cascaded converter control, and parallel connected converter control.

Wenli Yao received his B.S. and M.S degrees in electrical engineering from the School of Automation, Northwestern Polytechnical University, Xi'an, China in 2009 and 2012, respectively, where he is currently working toward his Ph.D. degree in power electronics. His research interests include current control, grid-connected inverter, multipulse converter, and power decoupling.

Hang Yin was born in Xi'an, China, in 1985. He received his B.S. and M.S. degrees in electrical engineering from Northwestern Polytechnical University, Xi'an, China in 2009 and 2012, respectively. He is currently working toward his Ph.D. degree in the Power Electronics Group, Institute of Energy and Automation Technology, Technology University of Berlin, Germany. His main research interests include medium voltage multilevel converter control for renewable energy integration.